Carbohydrate Polymers 117 (2015) 610–615

Contents lists available at ScienceDirect

Carbohydrate Polymers

journal homepage: www.elsevier.com/locate/carbpol

# Self-assembled nanoparticles of acetylated cashew gum: Characterization and evaluation as potential drug carrier

Nadia A.O. Pitombeira[a], José Guilherme Veras Neto[a], Durcilene A. Silva[b], Judith P.A. Feitosa[a], Haroldo C.B. Paula[c], Regina C.M. de Paula[a,*]

[a] Depto de Química Orgânica e Inorgânica—UFC—CEP, Caixa Postal 6021–R. Humberto Monte s/n, Campus do Pici, 60455-760 Fortaleza, Brazil
[b] Departamento de Ciências do Mar-UFPI, Parnaiba Brazil
[c] Departamento de Química Analítica e Físico-Química–UFC, Fortaleza, Brazil

ARTICLE INFO

*Article history:*
Received 30 April 2014
Received in revised form
24 September 2014
Accepted 25 September 2014
Available online 16 October 2014

*Chemical compounds studied in this article:*
Indomethacin (CID: 3715)
Formamide (CID: 713)
Pyridine (CID: 1049)
Acetic anhydride (CID: 7918)
Dimethyl sulfoxide (CID: 679)

*Keywords:*
Hydrophobic cashew gum
Acetylation
Hydrophobic polysaccharide
Nanoparticle
Drug release
Indomethacin

ABSTRACT

Acetylated cashew gum (ACG) was synthesized and self-assembled nanoparticles were obtained through the dialysis of an organic solution (DMSO) against a non-solvent (water). The ACG was characterized by infrared spectroscopy. The degree of substitution was 2.8 as determined by NMR spectroscopy. The physicochemical properties of the self-assembled nanoparticles in aqueous media were characterized by DLS, SEM and fluorescence spectroscopy. The mean diameter of the self-assembled nanoparticles obtained was 179 nm and the critical aggregation concentration (CAC) in water was $2.1 \times 10^{-3}$ g/L. Indomethacin (IND) was used as a hydrophobic model drug and was incorporated into the hydrophobized polysaccharide. Both loaded and unloaded nanoparticles were found to be spherical with diameters in the ranges of 70–170 nm and 108–314 nm (determined by SEM), respectively. Controlled drug release was observed for up to 72 h.



## 1. Introduction

Progressively increasing interest has been focused on self-assembled nanoparticles obtained from hydrophobized water-soluble polymers due to their potential biomedical and pharmaceutical applications (Ding, Richter, Matuana, & Heiden., 2011; Gonçalves & Gama, 2008; Jeong et al., 2006; Na, Lee, & Bae, 2003; Tan et al., 2011; Zhang et al., 2009). Hydrophobized or hydrophobic polymers can self-assemble in aqueous solution forming nanoparticles. In this context, amphiphilic block copolymers and hydrophobized polymers have been previously synthesized and their structure-function relationships studied (Ding et al., 2011; Lee et al., 2012; Na et al., 2003; Suksiriworapong, Sripha, Kreuter, & Junyaprasert, 2012; Park, Park, & Na, 2010; Pawar & Edgar, 2012).

Nanoparticulate drug delivery systems seem to represent a viable and promising strategy for the biopharmaceutical industry. They can increase the bioavailability, solubility and permeability of many potent drugs which are otherwise difficult to deliver orally (Kumari, Yadav, & Yadav, 2010). The nanometer size ranges of such systems offer certain distinct advantages, such as the possibility of penetrating deep into tissues through fine capillaries (*e.g.*, liver), and they are generally taken up efficiently by the cells (Vinagradov, Bronich, & Kabanov, 2002). Polysaccharides, being hydrophilic, can be modified with hydrophobic molecules or oligomers, resulting in amphiphilic biopolymers, which can self-assemble in water forming nanoparticles or nanogels, which are useful for drug delivery applications.

The use of self-assembled polysaccharides as drug delivery systems has recently been reviewed (Hassani, Hendra, & Bouchemal, 2012). Hydrophobized polysaccharides such as cellulose (Horning

* Corresponding author. Tel.: +55 85 33669979; fax: +55 8533669978.
*E-mail address:* rpaula@dqoi.ufc.br (R.C.M. de Paula).

http://dx.doi.org/10.1016/j.carbpol.2014.09.087
0144-8617/

& Heinze, 2008; Lucero, Claro, Casas, & Jimenez-Castellanos, 2013), dextran (Hassani et al., 2012; Aumelas, Serrero, Durand, Dellacherie, & Leonard, 2007; Hornig, Bunjes, & Heinze, 2009; Nichifor, Lopes, Carpov, & Melo, 1999), pullulan (Lee et al., 2012; Zhang et al., 2009), chondroitin sulfate (Park et al., 2010), chitosan (Hassani et al., 2012; Hwang, Kim, Kwon, & Kim, 2008), hyaluronic acid (Surace et al., 2009), amylose (Lalush, Bar, Zakaria, Eichler, & Shimoni, 2005), heparin (Park et al., 2004) and curdlan (Na, Park, Kim, & Bae, 2000), amylopectin (Lu, Zhang, Wang, & Chen, 2011) alginate (Shi, Zhang, Qi, & Cao, 2012; Pawar & Edgar, 2012) have been used for the formation of self-assembling nanoparticles with a view to their application as drug carriers.

The hydrophobic groups are covalently linked to the polysaccharide and can be polymer or small hydrophobic segments. Poly(alkylcyanoacrylates) and poly(methyl methacrylates) are examples of polymeric hydrophobic groups (Vauthier & Bouchemal, 2009). Oleoyl chloride, carboxylic acid (cholic and deoxycholic acids), acid anhydrides (acetic, propionic, *n*-butyric, *n*-valeric, hexanoic, octanoic, lauric, palmitic and stearic) and cholesterol are some of the small molecules used for polysaccharide hydrophobization (Hassani et al., 2012).

Cashew gum (CG) is a polysaccharide extracted from a low cost and easily available source, the *Anacardium occidentale* tree, widely distributed in the northeast of Brazil. According to the IBGE, in 2006, cashew trees covered an area of 710,404 hectares. The exudation of the gum occurs easily and often spontaneously. The average production is 700 g gum/plant/year (Bandeira, 1991). Taking into account that the average density is 100 plants/hectare, a production 50,000 t gum/year is possible, which is sufficient to supply many industrial applications. The gum is reported to contain, in wt.%, β-D-galactose (72–73%), α-D-glucose (11–14%), α-D-arabinose (4.6–5%), α-D-rhamnose (3.2–4%) and β-D-glucuronic acid (4.7–6.3%) (Rodrigues & de Paula, 1995; de Paula, Heatley, & Budd, 1998). The GC polysaccharide is composed by a main chain of β-D-galactose 1→3 linked with side chains of galactose and glucose. The other monosaccharides are present as terminal units (de Paula et al., 1998).

Indomethacin (IND), a non-steroidal anti-inflammatory drug, was chosen as the model drug due to its hydrophobic characteristics. The aim of this study was the production and characterization of self-assembled nanoparticles from hydrophobized cashew gum containing IND as a model drug and the evaluation of its release profile as a proof-of-concept for a drug delivery device.

## 2. Material and methods

### 2.1. Materials

Crude CG samples were collected from native trees in Fortaleza, Ceará, Brazil. They were purified as a sodium salt ($M_w = 1.8 \times 10^5$ g/mol) using a previously described method (de Paula et al., 1998). Indomethacin was purchased from Evidence Pharmac. All other reagents were of analytical grade (Formamide, pyridine, acetic anhydride, dimethyl sulfoxide were purchase from Vetec and pyrene was obtained from Fluka).

### 2.2. Cashew gum acetylation

In order to induce amphiphilic properties, acetyl moieties were chemically introduced into cashew gum polysaccharide using the methodology proposed by Motozato, Ihara, Tomoda, and Hirayama (1986). Cashew gum (1 g) was suspended in 20 mL of formamide and dissolved with vigorous stirring at 50 °C. Pyridine (6 mL) and acetic anhydride (15 mL) were added and the mixture was stirred for 24 h. Acetylated cashew gum (ACG) was precipitated with 400 mL of water, filtered, washed with water and dried in hot air.

### 2.3. Preparation of self-assembled nanoparticles

The ACG (20 mg) was dissolved in 20 mL of dimethyl sulfoxide (DMSO) and the solution was dialyzed (molecular weight cut-off 14 kD) against distilled water. The end of dialysis was determined when the conductance of the outside water became equal to that of the distilled water (after 3 days). The dialyzeted solution was filtered with a 0.45 μm syringe filter in order to remove dust and precipitants and ACG solid was recovered by freeze drying.

### 2.4. Critical aggregation concentration (CAC)

The CAC of the acetylated cashew gum was determined by fluorescence spectroscopy using pyrene as the fluorescence probe (Jung, Jeong, & Kim, 2003; Park et al., 2007). The ACG (20 mg) was dissolved in 20 mL of DMSO and the solution was dialyzed against water. The resultant suspension was diluted to give various nanoparticle concentrations. A stock solution of pyrene in acetone ($6 \times 10^{-6}$ mol/L, 1 mL) was added to different nanoparticle suspension concentrations (final volume 10 mL) to give a final pyrene concentration of $6 \times 10^{-7}$ mol/L. The fluorescence intensity was measured in a fluorescence spectrometer (Hitachi, F4500) applying an emission wavelength of 390 nm. The excitation and emission bandwidths were both 5 nm.

### 2.5. Indomethacin loading and in vitro release studies

Indomethacin loaded nanospheres were prepared as follows: ACG (180 mg) and indomethacin (20 mg) were dissolved in DMSO, dialyzed against water (molecular weight cut-off 14 kD) filtered and then freeze dried. To measure the drug loading content, 5 mg of IND loaded nanoparticles were dissolved in DMSO (10 mL) and stirred for 1 h. The indomethacin content was determined by UV absorption at 319 nm (Shimadzu UV 1800 spectrometer) and it was calculated using a IND calibration curve relating absorbance and concentration. The drug load (DL) was calculated according to the following equation (Park et al., 2010):

$$\mathrm{DL}(\%) = \frac{\text{mass of loaded IND}}{\text{mass of nanoparticles}} \times 100\% \quad (1)$$

*In vitro* drug release studies were carried out in triplicate as follows: 20 mg of the IND-loaded nanoparticles were introduced into dialysis bags (molecular weight cut-off 14 kD) which were placed in 20 mL of phosphate buffer solution (PBS), pH 7.4, at 37 °C with stirring (100 rpm). Aliquots (2 mL) of the samples were withdrawn periodically, replaced with an equal amount of fresh PBS, and the drug content was determined spectrophotometrically at 319 nm. The measurements of the absorbance at a wavelength were converted into the percentage of drug released according to a previously established calibration curve and confirmed linearity of the equation ($R = 0.999$).

### 2.6. Methods

#### 2.6.1. FT-IR spectroscopy

FT-IR spectra were recorded with KBr pellets on an FT-IR Shimadzu 8300 spectrophotometer in the range of 4000 to 400 $cm^{-1}$, with a resolution of 2 $cm^{-1}$ and 15 scans.

#### 2.6.2. Nuclear magnetic resonance

NMR spectra of 3% w/v solutions of derivative in DMSO-$d_6$ were recorded at 353 K on a Fourier transform Bruker Avance DRX 500 spectrometer with an inverse multinuclear gradient probe-head

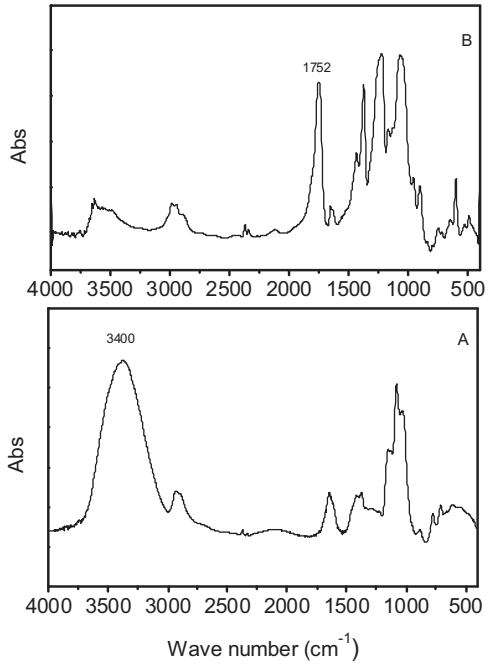


**Fig. 1.** FTIR spectra for cashew gum (A) and ACG (B).

equipped with z-shielded gradient coils and a Silicon Graphics workstation. Sodium 2,2-dimethylsilapentane-5-sulphonate (DSS) was used as the internal standard (0.00 ppm for $^1$H).

*2.6.3. Scanning electron microscopy (SEM)*

The scanning electron microscopy was recorded using a Jeol-6360LV field emission microscope. To prepare the SEM sample, a drop of the nanoparticle suspension was deposited on double-stick carbon tape on aluminum stubs, dried and coated with gold.

*2.6.4. Particle size measurements and zeta potential*

Particle size and zeta potential measurements were carried out on a Malvern Zetasizer Nano, Model ZS 3600, analyzer. The hydrodynamic diameter was measured by dynamic light scattering (DLS) with laser at a wavelength of 633 nm and a fixed scattering angle of 173°. Each sample was measured five times for three replicate samples. The particle size of the colloidal suspension was also monitored according to the time of storage at neutral pH.

## 3. Results and discussion

*3.1. Synthesis and characterization of hydrophobized cashew gum*

The FTIR spectra for CG and its derivative (ACG) are shown in Fig. 1. The gum showed a broad band at 3400 cm$^{-1}$ due to the stretching vibration of O—H, a small peak at 2933 cm$^{-1}$ attributed to the C—H stretching vibrations, and absorption at 1649 cm$^{-1}$ due to O—H scissor vibrations from bound water molecules (Bueno, 1990). Strong peaks at 1150, 1080 and 1030 cm$^{-1}$ are due to the stretching vibrations of C—O—C from glycosidic bonds and O—H bending of alcohols. The intensity of the stretching vibration of hydroxyl groups present in the CG at 3400 cm$^{-1}$ decrease in the ACG spectrum. The new absorption band due to C=O stretching vibrations at around 1750 cm$^{-1}$ verifies the insertion of acetyl groups in the cashew gum structure (Park et al., 2007).

Fig. 2 shows the $^1$H NMR spectra for the cashew gum and ACG in DMSO-$d_6$. The CG spectrum is very complex and the OH and H-1 to H-6 protons present in the polysaccharide are shown in the region

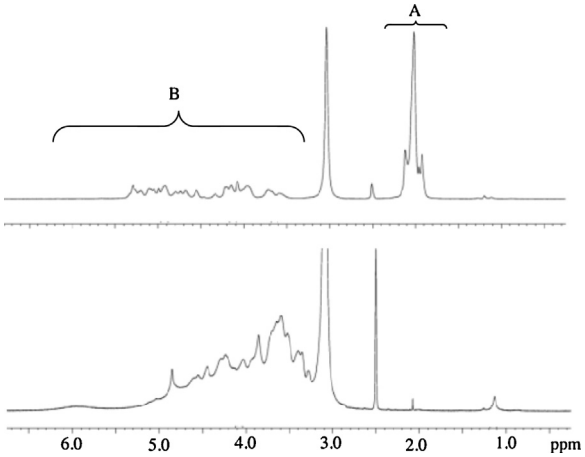


**Fig. 2.** $^1$H NMR spectra for cashew gum (CG) and ACG.

from 3.5 to 4.9 ppm. The signal at 1.1 ppm is due to $CH_3$ of rhamnose. The ACG spectrum shows new signals in 1.8–2.2 ppm due to acetyl protons. The degree of substitution (DS) of acetyl groups was calculated as proposed by Teramoto and Shibata (2006). The DS value is given by the following equation:

$$DS = \frac{10A}{(3B + A)} \quad (2)$$

where $A$ is the integral area of acetyl protons at 1.8–2.2 ppm and $B$ is the integral value for OH and H-1 to H-6 polysaccharide protons observed at >3.5 ppm.

The degree of substitution (DS) obtained for the derivative (ACG) was 2.8. Pullulan was acetylated using pyridine and acetic anhydride and the DS observed range from 3.00 to 2.71 (Zhang et al., 2009). Pullulan acetate with DS ranging from 1.0 to 3.0 were obtained using acetyl chloride in presence of pyridine (Teramoto & Shibata, 2006).

The $^{13}$C NMR spectrum for ACG in DMSO-$d_6$ is shown in Fig. 3. ACG spectrum shows signals due anomeric carbons in the range of 90–110 ppm, primary and ring carbons in the region of 60 to 85 ppm and $CH_3$ of rhamnose at 17.5 ppm This signals are due monosaccharides present in cashew gum. The signals previously described are similar to signals observed in the spectrum of CG using $D_2O$ as the solvent (de Paula et al., 1998). The very low intensity signal at 175.7 ppm attributed by de Paula et al. (1998) as carbonyl group of glucuronic acid in CG spectrum was not detected in ACG spectrum. In the ACG spectrum new signals at 169–168 ppm due to carbonyl groups and at 19.8–19.5 ppm due to methyl groups of acetate confirm the formation of hydrophobized acetate cashew gum.

*3.2. Preparation and characterization of self-assembled nanoparticles obtained from acetylated cashew gum*

Acetylated nanoparticles were prepared by dialysis methods using DMSO as the initial solvent. The formation of nanoparticles

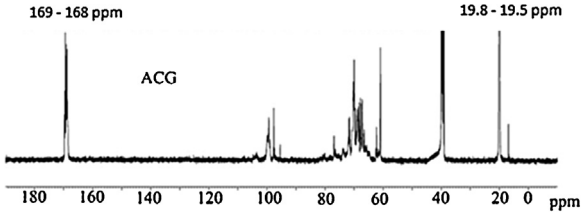


**Fig. 3.** $^{13}$C NMR spectrum for ACG sample.

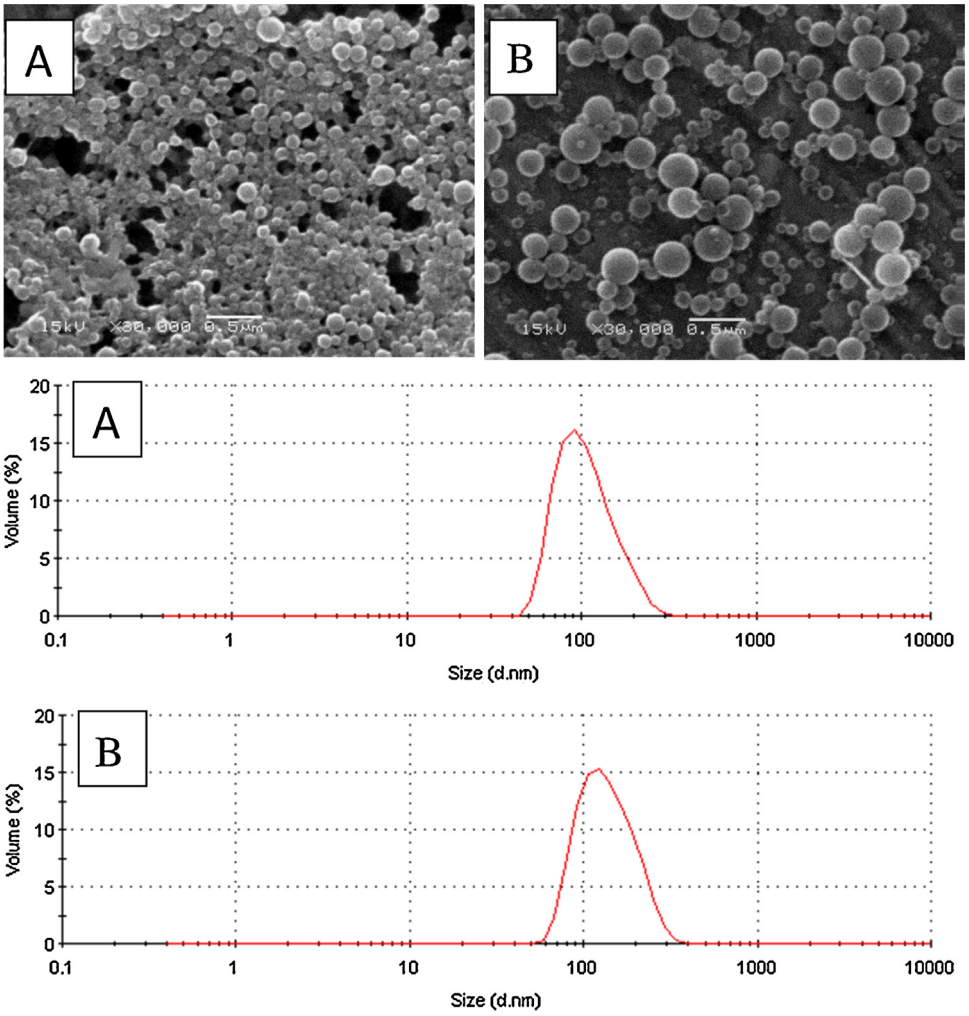


**Fig. 4.** Particle size distribution (determined by DLS) and SEM images of ACG nanoparticles without (A) and with IND (B).

during dialysis is based on the slow exchange of the organic solvent with the non-solvent water. The particle size was obtained by dynamic light scattering and a unimodal particle size distribution was observed. The average particle size was 179 and 140 nm, respectively, for unloaded and indomethacin loaded ACG nanoparticles (Fig. 4). The polydispersive index for unloaded (0.113) and IND load nanoparticles (0.117) indicate good particle size distribution. Colloidal stability is observed for zeta potential values above 30 mV in modulus The IND-loaded nanoparticles showed a higher value (in modulus) for the zeta potential (−47 mV) compared to the unloaded nanoparticles (−30.1 mV), indicating a more stable colloid system (Mohanraj & Chen, 2006).

The colloidal stability of the ACG nanoparticles was monitored over a one year period The ACG nanoparticle colloidal dispersion was very stable with no detectable changes in the particle size after one year of storage, which may be associated with the zeta potential value observed for this sample.

SEM images (Fig. 4) for the ACG and IND-loaded ACG nanoparticles show spherical particles. The sizes determined by SEM were in the ranges of 108–314 nm and 70–170 nm for ACG and IND-loaded ACG nanoparticles, respectively. The smaller particles in the latter case may be due to the formation of a more hydrophobic core leading to particle contraction.

Self-assembly behavior of ACG in aqueous media was investigated by fluorescence in the presence of pyrene as a probe. Fig. 5A shows the fluorescence excitation spectra of the CG derivative (ACG) at different concentrations in the presence of pyrene at $6.0 \times 10^{-7}$ mol/L. The fluorescence of the pyrene increases with increasing ACG concentration.

The critical aggregation concentration (CAC) can be determined by plotting the intensity ratio ($I_{337}/I_{334}$) of pyrene *vs.* ACG concentration. The CAC value can be obtained from the crossover point at low concentration for each sample and was $2.1 \times 10^{-3}$ g/L (Fig. 5B). This CAC value is lower than those previously observed for carboxymethyl curdlan substituted with sulfonylurea ($1.89 \times 10^{-2}$–$4.23 \times 10^{-2}$ g/L) (Na et al., 2000), but higher than those obtained for a pullulan acetate derivative ($3–5 \times 10^{-4}$ g/L) (Jung et al., 2003). Chitosan grafted with stearic acid formed micelles through self-association and the CACs ranged from 1.0 to $6.0 \times 10^{-2}$ g/L (Hu et al., 2006;) while dextran grafted with cholic acid, with a DS of 4%, showed a CAC of $20.0 \times 10^{-2}$ g/L and an average particle size of 130 nm (Nichifor et al., 1999).

### 3.3. Indomethacin loading and in vitro release studies

The drug loading (DL) for the ACG nanoparticles was 46.7%. The indomethacin (IND) release profile (Fig. 6A) shows an initial burst effect in the first 2 h followed by a controlled release up to 72 h. The burst effect may be due to absorbed indomethacin onto nanoparticle surface. Similar result were observed using a pullulan graft poly (DL- lactide-*co*-glycolide) where a burst of hydrophobic drug was observed up to 1 day (Jeong et al., 2006). The release profile

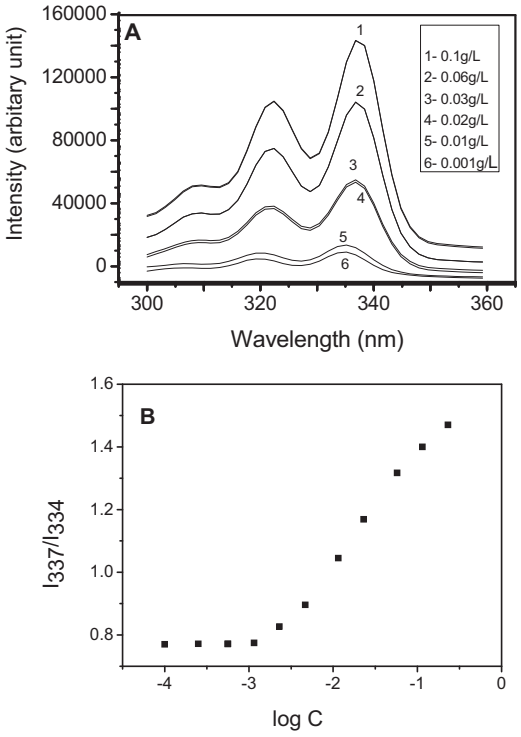


**Fig. 5.** Fluorescence excitation spectra for ACG (A) and plot of intensity ratio ($I_{337}/I_{334}$) of pyrene *vs.* ACG concentration (B).

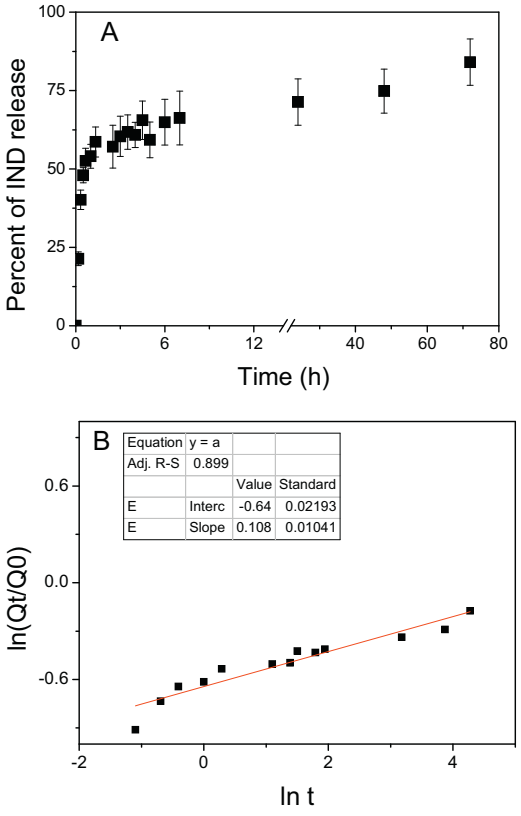


**Fig. 6.** *In vitro* drug release profiles for various drug-loaded ACG nanoparticles (pH 7.4, 37 °C) (A) and double-logarithmic plots of the cumulative drug release ($Q_t/Q_0$) as a function of time ($t$) for the drug-loaded nanoparticles (B).

observed is not due to the dialyze membrane effect as a control experiment shows that 84% indomethacin released in 2 h (data show in supplementary file). According to the literature, hydrophobized alginate with IND loading as high as 75.6% presented a release of *circa* 60% within 12 h, and the authors noted that the insertion of hydrophobic groups into the alginate decreased the drug release (Shi et al., 2012). In another study, hydrophobized amylopectin presented lower released values of 20.0–46.0% IND over 8 h (Lu et al., 2011).

To understand the mechanism of the indomethacin release from the ACG nanoparticles, data from the curves of Fig. 6A were fitted applying the following equation (Korsmeyer & Peppas, 1981):

$$\frac{Q_t}{Q_0} = k \ \ t^n \tag{3}$$

where $Q_t$ is the amount of drug released in time $t$, $Q_0$ is the initial amount of drug in the sample, $k$ is the release constant, and $n$ is the release exponent. For spherical forms, the $n$ exponent may explain the following release mechanisms: Fickian diffusion ($n \leq 0.43$), anomalous transport ($0.43 < n < 0.85$) and polymer swelling ($n \geq 0.85$) (Siepmann & Siepmann, 2008). Fig. 6B gives the plots of the cumulative drug release ($Q_t/Q_0$) as a function of time ($t$) for IND-loaded nanoparticles. The linear relationship observed, with a correlation coefficient ($R$) of >0.970, suggested that the *in vitro* release behavior could be described by the Korsmeyer–Peppas equation. For the drug-loaded ACG the $n$ value was found to be 0.43, characterizing Fickian diffusion where the rate of diffusion is less than that of relaxation. According to the literature, $n$ values of between 0.5 and 1.0 have been reported for hydrophobized amylopectin, indicating that the drug release occurs via an anomalous transport mechanism (Lu et al., 2011). The differences found may due to differences in aggregation due to different hydrophobic groups present in hydrophobized amylopectin and acetylated cashew gum

## 4. Conclusions

Acetylated cashew gum was successfully synthesized and self-assembled nanoparticles were produced by the dialysis method. Unimodal particle size distributions were observed using dynamic light scattering with an average size of 179 nm. The cashew gum derivative shows good colloidal stability, evaluated considering the particle size and size distribution over a storage period of one year. The SEM image shows spherical particles and a decrease in the size upon drug entrapment. An initial burst was observed in the first two hours followed by a controlled IND release up to 72 h.Acknowledgements

The authors gratefully acknowledge financial support from Rede Nanoglicobiotec (Nanoglicobiotec Network), INOMAT-INCT, CNPq, CAPES and FUNCAP and also Prof. Fernando Galembeck (Grupo de Morfologia e Topoquímica de Sólidos) from UNICAMP/Brazil for the SEM images.

## References

Aumelas, A., Serrero, A., Durand, A., Dellacherie, E., & Leonard, M. (2007). Nanoparticles of hydrophobically modified dextrans as potential drug carrier systems. *Colloids and Surfaces B: Biointerfaces*, *59*, 74–80.

Bandeira, C. T. (1991). *Relatório técnico da Empresa Brasileira de Pesquisa Agropecuária* (6) EMBRAPA., vol. 1.

Bueno, W. A. (1990). *Manual de Espectroscopia Vibracional*. São Paulo: McGraw-Hill.

de Paula, R. C. M., Heatley, F., & Budd, P. M. (1998). Characterization of *Anacardium occidentale* exudate polysaccharide. *Polymer International*, *45*, 27–35.

Ding, X., Richter, D. L., Matuana, L. M., & Heiden, P. A. (2011). Efficient one-pot synthesis and loading of self-assembled amphiphilic chitosan nanoparticles for low-leaching wood preservation. *Carbohydrate Polymers*, *86*, 58–64.

Gonçalves, C., & Gama, F. M. (2008). Characterization of the self-assembly process of hydrophobically modified dextrin. *European Polymer Journal*, *44*, 3529–3534.

Hassani, L. N., Hendra, F., & Bouchemal, K. (2012). Auto-associate amphiphilic polysaccharides as drug delivery systems. *Drug Discovery Today*, *17*, 608–614.
Horning, S., & Heinze, T. (2008). Efficient approach to design stable water-dispersable nanoparticles of hydrophobic cellulose esters. *Biomacromolecules*, *9*, 1487–1492.
Hornig, S., Bunjes, H., & Heinze, T. (2009). Preparation and characterization of nanoparticles based on dextran–drug conjugates. *Journal of Colloid and Interface Science*, *338*, 56–62.
Hu, F.-Q., Ren, G.-F., Yuan, H., Du, Y.-Z., Zeng, S., Hu, F-Q., et al. (2006). Shell cross-linked stearic acid grafted chitosan oligosaccharide self-aggregated micelles for controlled release of paclitaxel. *Colloids and Surfaces B: Biointerfaces*, *50*, 97–103.
Hwang, H-Y., Kim, I-S., Kwon, I. C., & Kim, Y-H. (2008). Tumor targetability and antitumor effect of docetaxel-loaded hydrophobically modified glycol chitosan nanoparticles. *Journal of Controlled Release*, *128*, 23–31.
Jeong, Y-I., Na, H-S., Oh, J-S., Choi, K-C., Song, C-E., & Lee, H-C. (2006). Adriamycin release from self-assembling nanospheres of poly(DL-lactide-*co*-glycolide)-grafted pullulan. *International Journal of Pharmaceutics*, *322*, 154–160.
Jung, S-. W., Jeong, Y-. I., & Kim, S-. H. (2003). Characterization of hydrophobized pullulan with various hydrophobicities. *International Journal of Pharmaceutics*, *254*, 109–121.
Korsmeyer, R. W., & Peppas, N. A. (1981). Effect of the morphology of hydrophilic polymeric matrices on the diffusion and release of water soluble drugs. *Journal of Membrane Science*, *9*, 211–227.
Kumari, A., Yadav, S. K., & Yadav, S. C. (2010). Biodegradable polymeric nanoparticles based drug delivery systems. *Colloids and Surfaces B: Biointerfaces*, *75*, 1–18.
Lalush, I., Bar, H., Zakaria, I., Eichler, S., & Shimoni, E. (2005). Utilization of amylose–lipid complexes as molecular nanocapsules for conjugated linoleic acid. *Biomacromolecules*, *6*, 121–130.
Lee, S. J., Hong, G.-Y., Jeong, Y., Kang, M-S., Oh, J.-S., Songd, C.-E., et al. (2012). Paclitaxel-incorporated nanoparticles of hydrophobized polysaccharide and their antitumor activity. *International Journal of Pharmaceutics*, *433*, 121–128.
Lu, H-W., Zhang, L-M., Wang, C., & Chen, R-F. (2011). Preparation and properties of new micellar drug carriers based on hydrophobically modified amylopectin. *Carbohydrate Polymers*, *83*, 1499–1506.
Lucero, M. J., Claro, C., Casas, M., & Jimenez-Castellanos, M. R. (2013). Drug diffusion from disperse systems with a hydrophobically modified polysaccharide: Enhancer® vs. Franz cells. *Carbohydrate Polymers*, *92*, 149–156.
Mohanraj, V. J., & Chen, Y. (2006). Nanoparticles—A review. *Tropical Journal of Pharmaceutical Research*, *5*, 561–573.
Motozato, Y., Ihara, H., Tomoda, T., & Hirayama, C. (1986). Preparation and gel permeation chromatographic properties of pullulan spheres. *Journal of Chromatography*, *355*, 434–437.
Na, K., Lee, K. H., & Bae, Y. H. (2003). Adriamycin loaded pullulan acetate/sulfonamide conjugate nanoparticles responding to tumor pH: pH-Dependent cell interaction, internalization and cytotoxicity *in vitro*. *Journal of Controlled Release*, *87*, 3–13.
Na, K., Park, H.-H., Kim, S. W., & Bae, Y. H. (2000). Self-assembled hydrogel nanoparticles from curdlan derivatives: characterization, anti-cancer drug release and interaction with a hepatoma cell line (HepG2). *Journal of Controlled Release*, *69*, 225–236.
Nichifor, M., Lopes, A., Carpov, A., & Melo, E. (1999). Aggregation in water of dextran hydrophobically modified with bile acids. *Macromolecules*, *32*, 7078–7085.
Park, K., Kim, K., Kwon, I. C., Kim, S. K., Lee, S., Lee, D. Y., et al. (2004). Preparation and characterization of self-assembled nanoparticles of heparin-deoxycholic acid conjugates. *Langmuir*, *20*, 11726–21173.
Park, K-. H., Song, H-. C., Na, K., Bom, H-S., Bae, Y. H., Lee, K. H., et al. (2007). *Colloids and Surfaces B: Biointerfaces*, *59*, 16–23.
Park, W., Park, S.-J., & Na, K. (2010). Potential of self-organizing nanogel with acetylated chondroitin sulfate as an anti-cancer drug carrier. *Colloids and Surfaces B: Biointerfaces*, *79*, 501–508.
Pawar, S. N., & Edgar, K. J. (2012). Alginate derivatization: A review of chemistry, properties and applications. *Biomaterials*, *33*, 3279–3305.
Rodrigues, J. F., & de Paula, R. C. M. (1995). Composition and rheological properties of cashew tree gum, the exudate polysaccharide from *Anacardium occidentale* L. *Carbohydrate Polymers*, *26*, 177–181.
Shi, J., Zhang, Z., Qi, W., & Cao, S. (2012). Hydrophobically modified biomineralized polysaccharide alginate membrane for sustained smart drug delivery. *International Journal of Biological Macromolecules*, *50*, 747–753.
Siepmann, J., & Siepmann, F. (2008). Mathematical modeling of drug delivery. *International Journal of Pharmaceutics*, *364*, 328–343.
Suksiriworapong, J., Sripha, K., Kreuter, J., & Junyaprasert, V. B. (2012). Functionalized (poly(-caprolactone)2-poly(ethylene glycol) nanoparticles with grafting nicotinic acid as drug carriers. *International Journal of Pharmaceutics*, *423*, 562–570.
Surace, C., Arpico, S., Dufaÿ-Wojcicki, A., Maraud, V., Bouclier, C., Clay, D., et al. (2009). Lipoplexes targeting the CD44 hyaluronic acid receptor for efficient transfection of breast cancer cells. *Molecular Pharmaceutics*, *6*, 1062–1073.
Tan, S., Zhao, D., Yuan, D., Wang, H., Tu, K., & Wang, L. (2011). Influence of indomethacin-loading on the micellization and drug release of thermosensitive dextran-graft-poly(*N*-isopropylacrylamide). *Reactive & Functional Polymers*, *71*, 820–827.
Teramoto, N., & Shibata, M. (2006). Synthesis and properties of pullulan acetate. Thermal properties, biodegradability, and a semi-clear gel formation in organic solvents. *Carbohydrate Polymer*, *63*, 476–481.
Vauthier, C., & Bouchemal, K. (2009). Methods for the preparation and manufacturing of polymeric nanoparticles. *Pharmaceutics Research*, *26*, 1025–1058.
Vinagradov, S. V., Bronich, T. K., & Kabanov, A. V. (2002). Nanosized cationic hydrogels for drug delivery: preparation, properties the blood- and interactions with cells. *Advanced Drug Delivery Reviews*, *54*, 223–233.
Zhang, H-Z., Gao, F-P., Liu, L-R., Li, X-M., Zhou, Z-M., Yang, X-D., et al. (2009). Pullulan acetate nanoparticles prepared by solvent diffusion method for epirubicin chemotherapy. *Colloids and Surfaces B: Biointerfaces*, *71*, 19–26.